FEBS Letters 587 (2013) 3928–3934

journal homepage: www.FEBSLetters.org

Eukaryotic translation initiation is controlled by cooperativity effects within ternary complexes of 4E-BP1, eIF4E, and the mRNA 5′ cap

Anna Modrak-Wojcik [a], Michal Gorka [a], Katarzyna Niedzwiecka [a,1], Konrad Zdanowski [b,c], Joanna Zuberek [a], Anna Niedzwiecka [a,d], Ryszard Stolarski [a,*]

[a] Division of Biophysics, Institute of Experimental Physics, Faculty of Physics, University of Warsaw, 93 Zwirki & Wigury St., 02-089 Warszawa, Poland
[b] Institute of Biochemistry & Biophysics, Polish Academy of Sciences, 5A Pawinskiego St., 02-106 Warszawa, Poland
[c] Institute of Chemistry, University of Natural Sciences and Humanities, 3 Maja 54 St., 08-110 Siedlce, Poland
[d] Laboratory of Biological Physics, Institute of Physics, Polish Academy of Sciences, 32/46 Lotnikow Ave., 02-668 Warszawa, Poland

ARTICLE INFO

Article history:
Received 22 July 2013
Revised 29 October 2013
Accepted 29 October 2013
Available online 6 November 2013

Edited by Michael Ibba

Keywords:
Translation initiation
4E-BP1
eIF4E
mRNA 5′cap
Analytical ultracentrifugation
Fluorescence

ABSTRACT

Initiation is the rate-limiting step during mRNA 5′ cap-dependent translation, and thus a target of a strict control in the eukaryotic cell. It is shown here by analytical ultracentrifugation and fluorescence spectroscopy that the affinity of the human translation inhibitor, eIF4E-binding protein (4E-BP1), to the translation initiation factor 4E is significantly higher when eIF4E is bound to the cap. The 4E-BP1 binding stabilizes the active eIF4E conformation and, on the other hand, can facilitate dissociation of eIF4E from the cap. These findings reveal the particular allosteric effects forming a thermodynamic cycle for the cooperative regulation of the translation initiation inhibition.

Structured summary of protein interactions:
4E-BP1 and eIF4E bind by cosedimentation in solution (View interaction)

1. Introduction

The central player in eukaryotic cap-dependent translation is the heterotrimeric eIF4F complex [1], responsible for recruitment of the small ribosomal subunit 40S. eIF4F is composed of the multifunctional eIF4G protein, the DEAD-box RNA helicase eIF4A and highly conserved eIF4E which is a primary anchor to the mRNA 5′ cap structure [2] (Scheme 1). This specific binding is a rate-limiting step for translation initiation [3]. eIF4G forms a bridge between eIF4E and the ribosome through other initiation factors and gives rise to mRNA circularization via an interaction with the poly(A)-binding proteins.

The eIF4E–eIF4G interface is a target of regulation by inhibitory proteins, 4E-BPs [4], that share a common eIF4E-binding motif with eIF4Gs [5]. Crystal structures of ternary complexes of eIF4E, a cap analogue, and the eIF4GII or 4E-BP1 peptide fragment revealed that both peptides bind eIF4E in the same manner, at the opposite side of eIF4E in relation to the cap-binding slot [6] (Scheme 1B). After mTOR-dependent hyperphosphorylation, 4E-BPs are no longer able to bind eIF4E [7] and the translation initiation can proceed [8].

eIF4E is overexpressed in tumour cells and its suppression inhibits the malignant transformation, thus targeting eIF4E may be promising in anti-cancer therapy [9]. Rational drug design aimed at eIF4E requires analysis of intermolecular interactions, including equilibrium association constants, K_{as}, which complement the static structural description of the crystal complexes, and provide us with the understanding of the protein dynamical behaviour in solution.

4E-BP1 is a natively disordered protein that partially folds upon association with eIF4E [10,11] which is, in turn, highly unstable in the *apo*-form [12–14]. This makes biophysical analyses of the interactions that rule the 4E-BP1/eIF4E/cap ternary complex non-

Abbreviations: eIF4E, eukaryotic initiation factor 4E; 4E-BP1, 4E binding protein 1; m^7GTP, 7-methylguanosine 5′-triphosphate; TCEP, tris (2-carboxyethyl) phosphine HCl; DB, dialysis buffer; SPR, surface plasmon resonance; TFA, trifluoroacetic acid

* Corresponding author. Fax: +48 22 55 40 771.
E-mail address: stolarsk@biogeo.uw.edu.pl (R. Stolarski).
[1] Present address: Institute of Biochemistry & Biophysics, Polish Academy of Sciences, 5A Pawinskiego St., 02-106 Warszawa, Poland.

0014-5793/$36.00
http://dx.doi.org/10.1016/j.febslet.2013.10.043

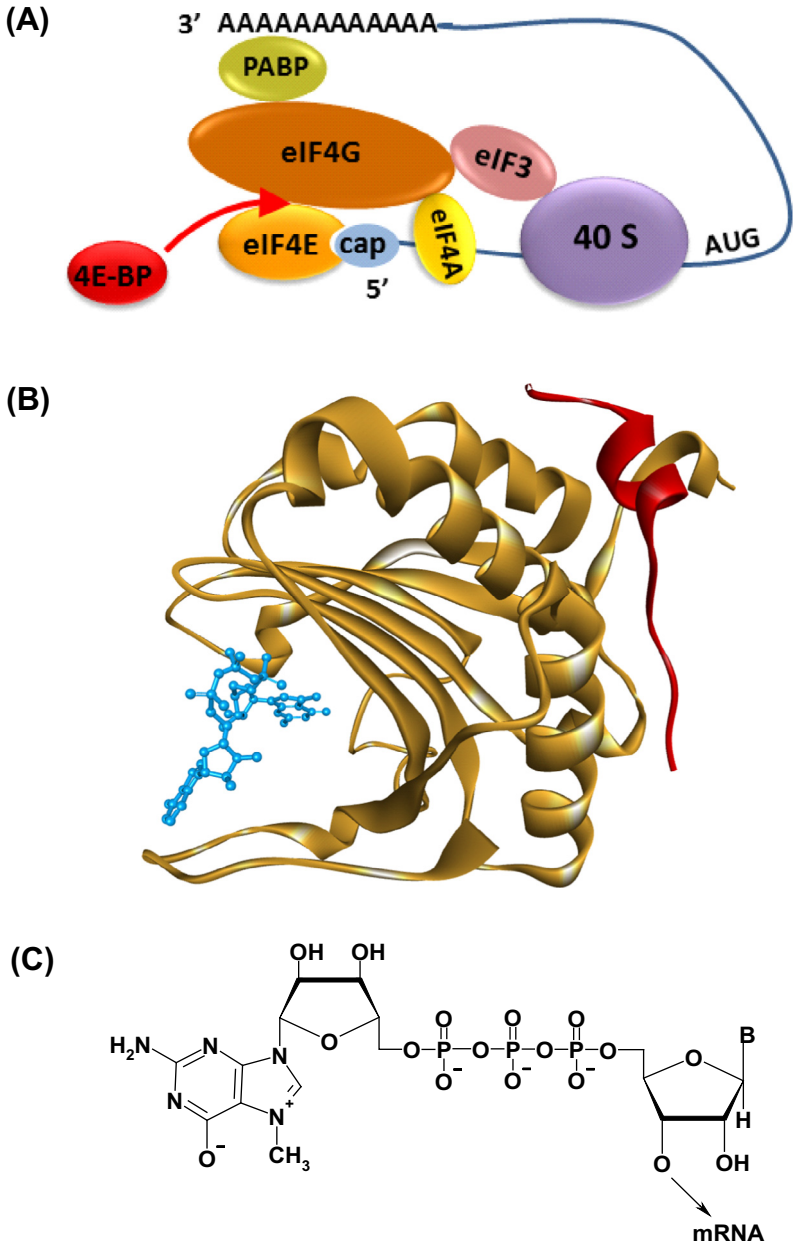

Scheme 1. (A) Scheme of the fragment of the translation preinitiation complex. Inhibitory activity of 4E-BP1 is marked as the red arrow. (B) Ternary complex of eIF4E (gold), m^7GpppA as the mRNA 5′ cap analogue (blue) and a fragment of 4E-BP1 (red) (1wkw [21]). (C) Chemical structure of the cap.

trivial, especially that the mutual influence of both binding sites must be taken into account.

Experimental data related to the influence of the cap on eIF4G and 4E-BP1 binding are scarce due to difficulty of working with *apo*-eIF4E. Our previous studies showed that the eIF4G/4E-BP1 binding site of eIF4E is more densely ordered when the protein is complexed with m^7GTP [15], in agreement with the NMR dynamics study [16]. We also revealed a 1.6-fold increase of eIF4GI(569–580) peptide affinity to cap-saturated eIF4E in comparison with the *apo*-protein, while no cooperativity was observed for 4E-BP1(51–67) that interacted with both eIF4E forms similarly, with K_{as} of 10^7 M^{-1} [12].

Conversely, the influence of eIF4G or 4E-BP1 on the eIF4E cap binding was more extensively elaborated. The pioneering SPR studies, accompanied by affinity column capacity measurements, were interpreted in terms of the eIF4E cap-affinity enhancement by 4E-BP1 [17]. The unambiguous eIF4E–cap complex stabilization was shown for larger fragments of eIF4G [18]. Accordingly, we reported a slightly higher association constants for m^7GTP binding by eIF4E saturated with eIF4GI and eIF4GII peptides, while, again, no cooperativity could be detected for 4E-BP1(51–67) [12].

Another open issue is related to the eIF4E-affinity for the 4E-BPs shorter fragments vs. the full-length proteins, since a direct comparison of the results obtained in solution and by surface-based methods, such as SPR, could be eligible only after satisfying strict SPR requirements within models providing for conformational changes [19]. Otherwise, such comparison could yield incoherent conclusions, especially that even the affinity values for the same complex formation and obtained within the same SPR protocol could differ thousands of times [20–25] (Supplementary Table).

To explain these puzzling data, we focus herein on interactions within the binary and ternary complexes of human full-length 4E-BP1 with eIF4E and the mRNA 5′ cap analogue. We apply analytical ultracentrifugation, both sedimentation velocity and equilibrium experiments, with rigorous fluorescence titration analysis [26] to elucidate intricate cooperative effects in the inhibited eIF4E–cap complex.

2. Materials and methods

m^7GTP was synthesised as described previously [27]. The concentration was determined spectrophotometrically on Jasco V-650 or Carry 100 Bio (Varian) spectrophotometers.

Human full-length eIF4E was expressed and purified as described earlier [28]. The final step was ion-exchange chromatography to remove misfolded molecules and aggregates (Supplementary Fig. 1). Gel filtration proved the eIF4E monomeric state (Supplementary Fig. 2). The samples were filtered through 0.45 μm syringe filters with FVDF membrane (ROTH). Total concentration of eIF4E was determined from absorption, ε_{280} 52 940 $cm^{-1}M^{-1}$ calculated using ProtParam [29].

Full-length 4E-BP1 was expressed in *Escherichia coli* BL21 (DE3) cells as the GST-fusion protein from the pGEX-6p1_h4E-BP1 plasmid, and purified using Glutathione Sepharose 4B bed (GE Healthcare) and Vydac C8 semi-preparative HPLC RP column as described in Supplementary Methods. 4E-BP1 concentration was determined from absorption, ε_{280} 2980 $cm^{-1}M^{-1}$ [29].

Analytical ultracentrifugation was run at 20 °C on Beckman Optima XL-I with 8-position An-Ti rotor and UV detection at 280 nm in a double-sector 1.2 cm cells with charcoal-filled epon centrepieces and sapphire windows.

Sedimentation velocity experiments were performed at 50 000 rpm. Radial absorption scans of protein concentration profiles were measured at 8-min intervals. Proteins were dialyzed twice against DB (50 mM HEPES/KOH buffer pH 7.2, 100 mM KCl and 0.1 mM TCEP), and 400 μl of the dialysate was loaded into reference sectors. Samples (390 μl) contained eIF4E at 4.3 μM, 4E-BP1 at 87 μM, or their mixtures containing 4E-BP1 at 0.5 μM to 45 μM. The solution of m^7GTP in DB was added to the suitable protein mixtures and to the reference to the final concentration of 5 μM. The sedimentation velocity data were analysed using program SEDFIT with a continuous sedimentation coefficient distribution model, $c(s)$, based on the Lamm equation [30,31]. To get the association constant for the eIF4E–4E-BP1 interaction, the $c(s)$ distributions were integrated to provide the weighted-average sedimentation coefficients as a function of 4E-BP1 concentration (s_w isotherm) [32]. The data was analysed by fitting 1:1 hetero-association model to the binding isotherm using SEDPHAT program [33]. For more details see Supplementary methods.

Sedimentation equilibrium experiments were performed at 21 000 rpm or for the multispeed experiments at 20 000, 25 000, and 30 000 rpm. Samples (110 μl) at the same concentrations as that for the velocity sedimentation experiments, and DB (120 μl) were placed in the cells. The radial concentration gradient was collected 10 times every 4 h at intervals of 0.001 cm, until the sedimentation equilibrium was attained (~30 h). The data were analysed by non-linear regression using SEDPHAT program, according to 1:1 hetero-association model and a global fitting to all experimental runs at various rotor speeds and eIF4E/4E-BP1 molar ratios [34] (see Supplementary methods).

Partial specific volumes of eIF4E and 4E-BP1, buffer density and viscosity were calculated using SEDNTERP program [35].

Fluorescence titrations of eIF4E at 0.15–0.25 μM, 20 °C, in 50 mM HEPES/KOH pH 7.2, 100 mM KCl, 1 mM dithiothreitol and 0.5 mM disodium ethylenediaminetetraacetate were performed as described previously [12,26] on Fluorolog Tau-3 (Horiba Jobin Yvon), in a thermostated quartz semi-micro cell (Hellma) with the optical length of 4/10 mm for excitation/emission, respectively. Aliquots of 1 μl m^7GTP at increasing concentrations, 2 μM to 1 mM, were added to 1400 μl of eIF4E. Excitation/emission wavelengths of 280/337 nm and 295/340 nm were applied with 1/4 nm spectral resolution and 4 s integration time. The excitation shutter was closed between measurements to avoid photobleaching. The fluorescence intensities were corrected for the *inner filter* effect, dilution and background, and analysed as a function of the total ligand concentration by non-linear, least-squares regression, using ORIGINPro 8 (Microcal Software Inc). Association constants, K_{as}, and concentrations of active eIF4E, P_{act}, were obtained as described previously [26,36]. Statistical analysis was done on the basis of runs tests and goodness of fit $R^2 > 0.99$.

3. Results and discussion

Since analytical ultracentrifugation is the method of choice to get reliable protein–protein binding constants without any covalent modifications of interacting species [37], we performed independent sedimentation velocity (Fig. 1) and sedimentation equilibrium (Fig. 2) experiments. Both types of the ultracentrifugation experiments could be performed for the interactions of eIF4E only with the full length 4E-BP1 and not with the short 4E-BP1 peptides, since the difference in sedimentation velocity and equilibrium for complexes with the latter and eIF4E alone are below the limit of detection.

Firstly, K_{as} determined by both methods for full-length 4E-BP1 binding to *apo*-eIF4E are in a perfect agreement (Table 1), and are very close (within 3σ) to the value for the short 4E-BP1(51–67) peptide, $\sim 10 \times 10^6\ M^{-1}$, obtained earlier by another highly reproducible, in-solution, equilibrium method, i.e., titration based on intrinsic fluorescence quenching of unmodified protein upon complex formation [7]. These suggest that the N- and C-terminal 4E-BP1 tails flanking the eIF4E-binding site do not play a role in recognition of *apo*-eIF4E. This observation is consistent with the NMR [10] and SAXS [11] data that showed partial folding and compaction of the 4E-BP1 central region containing the eIF4E-binding motif upon interaction with *apo*-eIF4E.

In contrast, while we did not observe any affinity changes of eIF4E to the 4E-BP1 short peptide after previous saturation of eIF4E with the mRNA 5′ cap analogue ($K_{as} \sim 10 \times 10^6\ M^{-1}$) [12], a significant, about 10-fold increase of the association constant for the

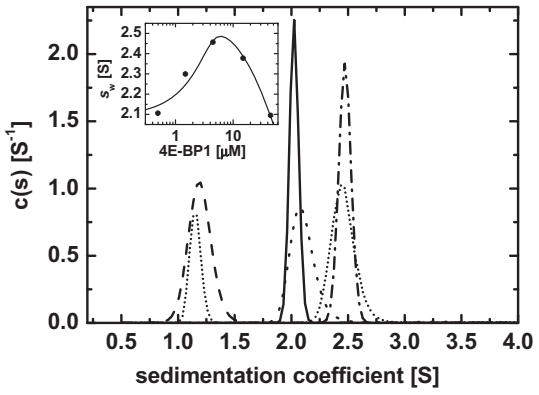

Fig. 1. Sedimentation velocity analysis of eIF4E–4E-BP1 interaction. Sedimentation coefficient distribution $c(s)$ of 4.3 μM *apo*-eIF4E (—), 87 μM *apo*-4E-BP1 (– –), and the mixture of 4.3 μM eIF4E with 4E-BP1 at 0.5 μM (- - -), 4.5 μM (— · —), and 45 μM (· · · ·). Inset: the weighted-average *s*-values (s_w) derived from integration of $c(s)$ as a function of 4E-BP1 concentration (●) and the best fit of the 1:1 hetero-association isotherm (—).

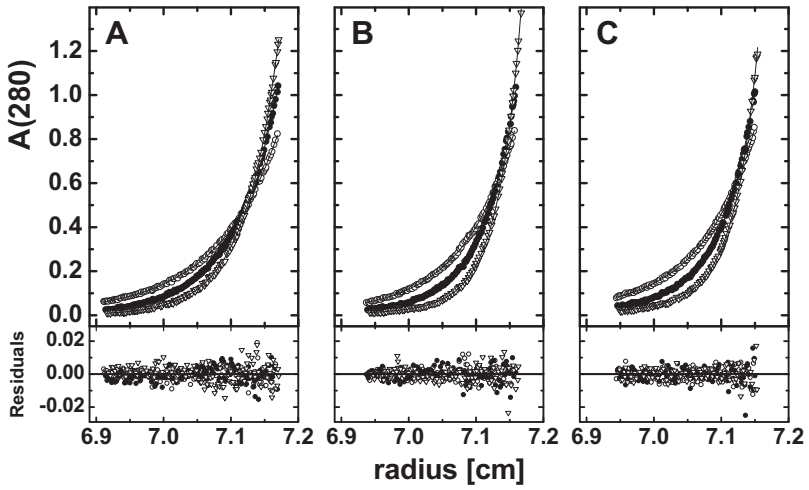

Fig. 2. Upper panels: sedimentation equilibrium gradients for mixtures containing 5 μM m^7GTP, 4.3 μM eIF4E, and 4E-BP1 at 0.6 μM (A), 7.5 μM (B), and 24 μM (C), for the rotor speeds of 20000 (o), 25000 (●), and 30000 rpm (▽) with the best global fits (—) of 1:1 hetero-association model. Bottom panels: fitting residuals.

Table 1
Equilibrium association constants, K_{as}, and binding free energies, $\Delta G°$, at 20 °C for formation of binary and ternary complexes of eIF4E with 4E-BP1 and the mRNA 5′ cap analogue, m^7GTP.

Titrating ligand	Preincubated ligand	K_{as} (μM^{-1})	$\Delta G°$ [kcal/mol]
Analytical ultracentrifugation			
4E-BP1	m^7GTP (μM)		
Sedimentation velocity experiments			
	0	6.18 ± 1.28	−9.10 ± 0.12
	5	58 ± 15	−10.41 ± 0.15
Sedimentation equilibrium experiments			
	0	6.34 ± 0.87	−9.12 ± 0.08
	5	52 ± 14	−10.35 ± 0.16
Fluorescence titration [a]			
m^7GTP	4E-BP1 (μM)		
	0	107.3 ± 5.0	−10.77 ± 0.03
	0.06	89.1 ± 7.0	−10.66 ± 0.05
	0.18	73.8 ± 2.9	−10.55 ± 0.02
	0.60	60.3 ± 3.2	−10.44 ± 0.03
	1.48	43.0 ± 3.9	−10.23 ± 0.05
	1.80	56.5 ± 3.1	−10.40 ± 0.03

[a] Fluorescence titrations of eIF4E at 0.17 μM with m^7GTP in the absence and presence of increasing concentrations of 4E-BP1.

inhibitor and the eIF4E–cap complex was found in case of the full-length 4E-BP1 (Table 1). This corresponds to the complex stabilization stronger by about −1.2 kcal/mol, which is a typical value of one non-covalent contact in water milieu. This enhanced interaction shows that full-length 4E-BP1 can detect the eIF4E conformational changes upon the cap binding, which confirms the previous studies that revealed the structural basis for the positive allosteric effect [15,16,38].

Functional significance of the N- and C-terminal 4E-BPs parts flanking the eIF4E-binding site was analysed earlier by binding studies for full-length 4E-BPs and their shorter fragments [24,25]. The data from which the conclusions were drawn varied significantly not only according to the applied method but also within the same approach (Supplementary Table). Our results show clearly that the N- and C-terminal 4E-BP1 regions play important role in formation of the complex with eIF4E only when the translation factor is already bound to the mRNA 5′ cap, but not in the case of the *apo*-eIF4E.

For small ligands binding, fluorescence titration was proved to be the most exact approach [12,26,36]. To our surprise, the precise values of the equilibrium association constants that we obtained for the cap binding to eIF4E after prior incubation with increasing concentrations of 4E-BP1 showed unambiguously that 4E-BP1 reduces the eIF4E-m^7GTP binding constant by ~50% (Fig. 3, Table 1). Apparently, this seems contradictory to the former results regarding greater amounts of eIF4E retained on the cap-affinity column in the presence of 4E-BPs [17]. However, this twofold decrease of K_{as}, at the high affinity of 10^8 M^{-1}, corresponds to weakening of the complex stability by 0.37 kcal/mol, i.e., only ~60% of the thermal energy, a negligible difference as for the m^7GTP-Sepharose affinity assay. Thus, the effect observed by us could not be revealed in the previous bed- and surface-supported experiments [17]. In fact, those greater quantities of eIF4E eluted from the cap-affinity column when bond to 4E-BP1 [17] could reflect the differences in the eIF4E fractions, i.e. the active fraction capable of interacting with the affinity bed. Earlier studies showed that 4E-BP1 stabilized the eIF4E structure by preventing proteolysis [13] and crystallization facilitation [39,40]. We have analysed quantitatively [26,36] the influence of 4E-BP1 on the active eIF4E concentration in the sample. Fig. 3D shows the clear and systematic increase of the active eIF4E fraction (i.e., capable of binding to the mRNA 5′ cap), from ~40% to ~93%, depending on the 4E-BP1 to eIF4E molar ratio in the identical eIF4E samples at a total concentration of 0.17 μM. The plateau is approached at the threefold excess of 4E-BP1, which corresponds to 94% saturation of eIF4E by 4E-BP1 in the presence of m^7GTP. This marked conformational stabilization effect exerted by 4E-BP1 on eIF4E is in agreement with the recent structural NMR findings that 4E-BP1 transforms eIF4E into a state, which is more susceptible for cap-binding [38] and with the conformational changes revealed earlier for the yeast eIF4E in the complex with the eIF4G fragment [41]. The over twofold increase of the active eIF4E concentration (Fig. 3D) resolves the apparent contradiction with McCarthy's group [17], since, statistically, over twice more eIF4E molecules can interact with the mRNA 5′ cap in the presence of 4E-BP1. Thus, naturally, more amount of eIF4E could be then retained on the m^7GTP-Sepharose [17].

Allosteric effects on the eIF4E-cap binding, common for full-length 4E-BP1 and eIF4G fragments, were also anticipated from the comparison of the X-ray diffraction and NMR data [38]. However, those suppositions were based only on, sometimes self-con-

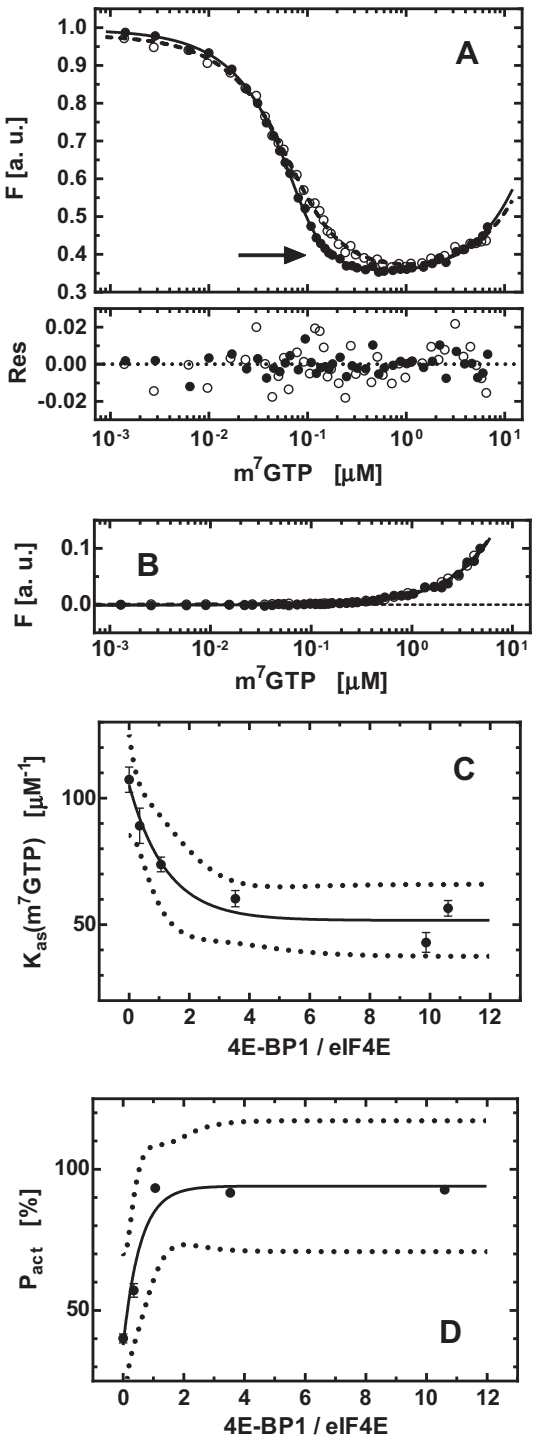

Fig. 3. eIF4E affinity to mRNA 5′ cap is down-regulated by 4E-BP1. (A) Binding isotherms from fluorescence titrations for interaction of m^7GTP with eIF4E at 0.15 μM in the *apo*-form (●), and in the presence of 1.5 μM 4E-BP1 (o), with the corresponding fitting residuals. The arrow points that saturation of *apo*-eIF4E with the cap occurs at lower concentrations than of eIF4E with 4E-BP1. (B) Control: pure buffer (●) and 1.5 μM 4E-BP1 (o) titrated with m^7GTP, proving that no interaction occurs between 4E-BP1 and m^7GTP. (C) Dependence of the eIF4E-m^7GTP association constant, K_{as}, and (D) of the amount of the active eIF4E, P_{act}, on the 4E-BP1/eIF4E molar ratio, with Boltzmann sigmoidal curve (—) and 95% confidence interval (· · ·).

tradictory, literature data without any affinity studies within one methodological approach. While the mutually positive allosteric effect of the yeast eIF4G or its fragments on the eIF4E–cap association was well documented [18,42,43], the human eIF4E-cap interaction was surprisingly shown to be unaffected by the presence or absence of the eIF4E-binding domain of eIF4G and vice versa [44].

Moreover, modulation of the eIF4E biological activity by 4E-BPs and eIF4Gs can be variant, despite the local secondary structure similarity of their eIF4E-bound short helical fragments [6]. It was shown previously that the image of interactions within ternary complexes including eIF4E, 4E-BP1 or eIF4G short peptides, and a cap analogue was unsymmetrical [12], since binding of one ligand influenced the eIF4E affinity to the other, but this was not necessarily accompanied by the evident effect in the reverse direction. Here, we have revealed an intricate cooperativity between the two eIF4E binding sites. The cumulative Gibbs free energy of the eIF4E binding to the cap and then to 4E-BP1 equals -21.15 ± 0.12 kcal/mol, while the binding constants describing the ternary complex formation in the reverse order lead to the value of $\Delta G^\circ = -19.51 \pm 0.08$ kcal/mol (Table 1, Scheme 2). Since the Gibbs free energy difference between this two pathways exceeds three standard deviations, this could suggest that another internal equilibrium process related to a conformational rearrangement of the eIF4E/4E-BP1 complex upon the cap binding might take place that is neither reflected by measurable intrinsic fluorescence changes nor by ultracentrifugation. This process would be related to ΔG° of ~1.64 kcal/mol (which is ~3 kT; thermal energy at 20 °C) and correspond to the conformational equilibrium constant, K_{eq} of 16.7. This relatively low value means that more that 5% of the ternary complex population could be present as the less stable (eIF4E/4E-BP) cap intermediate (Scheme 2). The results can be interpreted as a kind of a thermodynamic cycle, as follows: the mRNA 5′ cap binding makes the affinity of eIF4E to full length 4E-BP1 significantly stronger, and then the binding of 4E-BP1 to the cap/eIF4E complex makes the cap dissociation slightly easier, since the association constant for the cap binding to eIF4E/4E-BP is twice lower than to eIF4E alone.

Our results thus support the opposite functions of the translation repressors and the translation initiation factors, since it appears that translation could be additionally inhibited by 4E-BP1 via facilitation of eIF4E dissociation from the mRNA 5′ cap in the living cell within a kind of a negative feedback loop.

It was interesting to consider the possibility of competition between the full length 4E-BP1 (118 residues) and the eIF4E-binding domain of eIF4G (90 residues) to eIF4E. The affinity of the eIF4G fragment to eIF4E was determined by SPR in the low nanomolar range, both for the human [44] and yeast [41] proteins. The equilibrium association constant for the human eIF4G–eIF4E complex, ca. 230×10^6 M^{-1} [44], is 35-fold greater than for the binding of 4E-BP1 to *apo*-eIF4E and still fourfold greater than in the case of the cap-bound eIF4E (Table 1). Bearing in mind that surface-based measurements may not always be compared directly to the equilibrium solution studies, one may cautiously conclude that the affinity of 4E-BP1 to eIF4E in the complex with the mRNA 5′ cap approaches to the strength of the eIF4E–eIF4G interaction.

The 4E-BP repressors are important mediators of mTORC1 regulatory function in cell growth and proliferation [45]. Most of the former investigations were focused on eIF4E affinity regulation by multiple 4E-BP phosphorylations, but the mechanism of translation inhibition by non-phosphorylated 4E-BPs can also be influenced by cooperativity between the cap- and eIF4G/4E-BP-binding sites. Based on the consistent quantitative studies, we have demonstrated for the first time that eIF4E bound to the mRNA 5′ cap comes under more strict control by full length 4E-BP1, which is accomplished by blocking the eIF4G-binding site with the association constant by one order of magnitude greater than that for *apo*-eIF4E. We have also explained that the biophysical origin of the observed 4E-BP1 influence on the eIF4E–cap binding is related

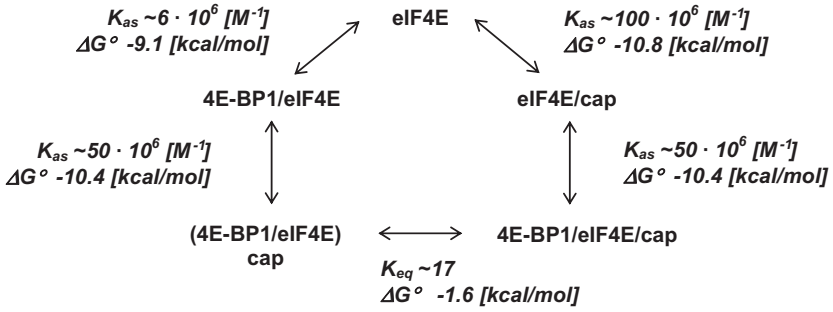

Scheme 2. Cap–eIF4E–4E-BP1 binding thermodynamic cycle.

to stabilization of the proper eIF4E conformation, accompanied by a slight decrease of the eIF4E–cap association constant.

Acknowledgments

This work was supported by Polish Ministry of Science and Higher Education (National Science Centre) Grant Nos. N301035936 and N301096339 (to J.Z.). We thank Prof. Nahum Sonenberg for the 4E-BP1 plasmid and Dr. Elzbieta Bojarska for help in 4E-BP1 purification. The analytical ultracentrifugation experiments were performed in the NanoFun laboratories, ERDF Project POIG.02.02.00-00-025/09.

Appendix A. Supplementary data

Supplementary data associated with this article can be found, in the online version, at http://dx.doi.org/10.1016/j.febslet.2013.10.043.

References

[1] Gebauer, F. and Hentze, M.W. (2004) Molecular mechanisms of translational control. Nat. Rev. Mol. Cell Biol. 5, 827–835.
[2] Topisirovic, I., Svitkin, Y.V., Sonenberg, N. and Shatkin, A.J. (2011) Cap and cap-binding proteins in the control of gene expression. RNA 2, 277–298.
[3] Gingras, A.C., Raught, B. and Sonenberg, N. (1999) EIF4 initiation factors: effectors of mRNA recruitment to ribosomes and regulators of translation. Annu. Rev. Biochem. 68, 913–963.
[4] Sonenberg, N. and Hinnebusch, A.G. (2009) Regulation of translation initiation in eukaryotes: mechanisms and biological targets. Cell 136, 731–745.
[5] Mader, S., Lee, H., Pause, A. and Sonenberg, N. (1995) The translation initiation factor eIF-4E binds to a common motif shared by the translation factor eIF-4 gamma and the translational repressors 4E-binding proteins. Mol. Cell Biol. 15, 4990–4997.
[6] Marcotrigiano, J., Gingras, A.C., Sonenberg, N. and Burley, S.K. (1999) Cap-dependent translation initiation in eukaryotes is regulated by a molecular mimic of eIF4G. Mol. Cell 3, 707–716.
[7] Gingras, A.-C., Raught, B., Gygi, S.P., Niedzwiecka, A., Miron, M., Burley, S.K., et al. (2001) Hierarchical phosphorylation of the translation inhibitor 4E-BP1. Genes Dev. 15, 2852–2864.
[8] Gingras, A.C., Gygi, S.P., Raught, B., Polakiewicz, R.D., Abraham, R.T., Hoekstra, M.F., et al. (1999) Regulation of 4E-BP1 phosphorylation: a novel two-step mechanism. Genes Dev. 13, 1422–1437.
[9] Graff, J.R., Konicek, B.W., Carter, J.H. and Marcusson, E.G. (2008) Targeting the eukaryotic translation initiation factor 4E for cancer therapy. Cancer Res. 68, 631–634.
[10] Fletcher, C.M., McGuire, A.M., Gingras, A.C., Li, H., Matsuo, H., Sonenberg, N., et al. (1998) 4E binding proteins inhibit the translation factor eIF4E without folded structure. Biochemistry 37, 9–15.
[11] Gosselin, P., Oulhen, N., Jam, M., Ronzca, J., Cormier, P., Czjzek, M., et al. (2011) The translational repressor 4E-BP called to order by eIF4E: new structural insights by SAXS. Nucleic Acids Res. 39, 3496–3503.
[12] Niedzwiecka, A., Marcotrigiano, J., Stepinski, J., Jankowska-Anyszka, M., Wyslouch-Cieszynska, A., Dadlez, M., et al. (2002) Biophysical studies of eIF4E cap-binding protein: recognition of mRNA 5′ cap structure and synthetic fragments of eIF4G and 4E-BP1 proteins. J. Mol. Biol. 319, 615–635.
[13] Tomoo, K., Shen, X., Okabe, K., Nozoe, Y., Fukuhara, S., Morino, S., et al. (2003) Structural features of human initiation factor 4E, studied by X-ray crystal analyses and molecular dynamics simulations. J. Mol. Biol. 328, 365–383.
[14] Niedzwiecka, A., Darzynkiewicz, E. and Stolarski, R. (2005) Thermodynamics and conformational changes related to binding of eIF4E protein to mRNA 5′ cap. J. Phys. Condens. Matter 17, S1483–S1494.
[15] Rutkowska-Wlodarczyk, I., Stepinski, J., Dadlez, M., Darzynkiewicz, E., Stolarski, R. and Niedzwiecka, A. (2008) Structural changes of eIF4E upon binding to the mRNA 5′ monomethylguanosine and trimethylguanosine Cap. Biochemistry 47, 2710–2720.
[16] Volpon, L., Osborne, M.J., Topisirovic, I., Siddiqui, N. and Borden, K.L.B. (2006) Cap-free structure of eIF4E suggests a basis for conformational regulation by its ligands. EMBO J. 25, 5138–5149.
[17] Ptushkina, M., von der Haar, T., Karim, M.M., Hughes, J.M. and McCarthy, J.E. (1999) Repressor binding to a dorsal regulatory site traps human eIF4E in a high cap-affinity state. EMBO J. 18, 4068–4075.
[18] Von Der Haar, T., Ball, P.D., Mccarthy, J.E.G. and von Der Haar, T. (2000) Stabilization of Eukaryotic Initiation Factor 4E Binding to the mRNA 5 -Cap by Domains of eIF4G∗. J. Biol. Chem. 275, 30551–30555.
[19] Myszka, D.G. (1997) Kinetic analysis of macromolecular interactions plasmon resonance biosensors. Curr. Opin. Biotechnol. 8, 50–57.
[20] Youtani, T., Tomoo, K., Ishida, T., Miyoshi, H. and Miura, K. (2000) Regulation of human eIF4E by 4E-BP1: binding analysis using surface plasmon resonance. IUBMB Life 49, 27–31.
[21] Tomoo, K., Matsushita, Y., Fujisaki, H., Abiko, F., Shen, X., Taniguchi, T., et al. (2005) Structural basis for mRNA cap-binding regulation of eukaryotic initiation factor 4E by 4E-binding protein, studied by spectroscopic, X-ray crystal structural, and molecular dynamics simulation methods. Biochim. Biophys. Acta 1753, 191–208.
[22] Tomoo, K., Abiko, F., Miyagawa, H., Kitamura, K. and Ishida, T. (2006) Effect of N-terminal region of eIF4E and Ser65-phosphorylation of 4E-BP1 on interaction between eIF4E and 4E-BP1 fragment peptide. J. Biochem. 140, 237–246.
[23] Abiko, F., Tomoo, K., Mizuno, A., Morino, S., Imataka, H. and Ishida, T. (2007) Binding preference of eIF4E for 4E-binding protein isoform and function of eIF4E N-terminal flexible region for interaction, studied by SPR analysis. Biochem. Biophys. Res. Commun. 355, 667–672.
[24] Mizuno, A., In, Y., Fujita, Y., Abiko, F., Miyagawa, H., Kitamura, K., et al. (2008) Importance of C-terminal flexible region of 4E-binding protein in binding with eukaryotic initiation factor 4E. FEBS Lett. 582, 3439–3444.
[25] Paku, K.S., Umenaga, Y., Usui, T., Fukuyo, A., Mizuno, A., In, Y., et al. (2012) A conserved motif within the flexible C-terminus of the translational regulator 4E-BP is required for tight binding to the mRNA cap-binding protein eIF4E. Biochem. J. 441, 237–245.
[26] Niedzwiecka, A., Stepinski, J., Antosiewicz, J.M., Darzynkiewicz, E. and Stolarski, R. (2007) Biophysical approach to studies of cap-eIF4E interaction by synthetic cap analogues in: Methods Enzymol. (Lorsch, J., Ed.), pp. 209–245, Elsevier.
[27] Darzynkiewicz, E., Ekiel, I., Tahara, S.M., Seliger, L.S. and Shatkin, A.J. (1985) Chemical synthesis and characterization of 7-methylguanosine cap analogues. Biochemistry 24, 1701–1707.
[28] Zuberek, J., Kubacka, D., Jablonowska, A., Jemielity, J., Stepinski, J., Sonenberg, N., et al. (2007) Weak binding affinity of human 4EHP for mRNA cap analogs. RNA 13, 691–697.
[29] E. Gasteiger, C. Hoogland, A. Gattiker, S. Duvaud, M.R. Wilkins, R.D. Appel, et al., Protein Identification and Analysis Tools on the ExPASy Server, in: Walker John M. (Ed.), Proteomics Protoc. Handb., 2005: pp. 571–607.
[30] Schuck, P. (2000) Size-distribution analysis of macromolecules by sedimentation velocity ultracentrifugation and lamm equation modeling. Biophys. J. 78, 1606–1619.
[31] Dam, J. and Schuck, P. (2004) Calculating sedimentation coefficient distributions by direct modeling of sedimentation velocity concentration profiles. Methods Enzymol. 384, 185–212.
[32] Schuck, P. (2003) On the analysis of protein self-association by sedimentation velocity analytical ultracentrifugation. Anal. Biochem. 320, 104–124.
[33] Dam, J., Velikovsky, C.A., Mariuzza, R.A., Urbanke, C. and Schuck, P. (2005) Sedimentation velocity analysis of heterogeneous protein-protein interactions: Lamm equation modeling and sedimentation coefficient distributions c(s). Biophys. J. 89, 619–634.

[34] Vistica, J., Dam, J., Balbo, A., Yikilmaz, E., Mariuzza, R.A., Rouault, T.A., et al. (2004) Sedimentation equilibrium analysis of protein interactions with global implicit mass conservation constraints and systematic noise decomposition. Anal. Biochem. 326, 234–256.
[35] Hayes, D., Laue, T., Philo, J. (1995) Program Sednterp: Sedimentation Interpretation, Program.
[36] Niedzwiecka, A., Stepinski, J., Darzynkiewicz, E., Sonenberg, N. and Stolarski, R. (2002) Positive heat capacity change upon specific binding of translation initiation factor eIF4E to mRNA 5′ cap. Biochemistry 41, 12140–12148.
[37] Schuck, P. (2013) Analytical ultracentrifugation as a tool for studying protein interactions. Biophys. Rev. 5, 159–171.
[38] Siddiqui, N., Tempel, W., Nedyalkova, L., Volpon, L., Wernimont, A.K., Osborne, M.J., et al. (2012) Structural insights into the allosteric effects of 4EBP1 on the eukaryotic translation initiation factor eIF4E. J. Mol. Biol. 415, 781–792.
[39] Liu, W.Z., Zhao, R., McFarland, C., Kieft, J., Niedzwiecka, A., Jankowska-Anyszka, M., et al. (2009) Structural insights into parasite eIF4E binding specificity for m(7)G and m(2,2,7)G mRNA Caps. J. Biol. Chem. 284, 31336–31349.
[40] Liu, W., Jankowska-Anyszka, M., Piecyk, K., Dickson, L., Wallace, A., Niedzwiecka, A., et al. (2011) Structural basis for nematode eIF4E binding an m2,2,7G-Cap and its implications for translation initiation. Nucleic Acids Res. 39, 8820–8832.
[41] von der Haar, T., Oku, Y., Ptushkina, M., Moerke, N., Wagner, G., Gross, J.D., et al. (2006) Folding transitions during assembly of the eukaryotic mRNA cap-binding complex. J. Mol. Biol. 356, 982–992.
[42] Gross, J.D., Moerke, N.J., der Haar, T., Lugovskoy, A.A., Sachs, A.B., McCarthy, J.E.G., et al. (2003) Ribosome loading onto the mRNA cap is driven by conformational coupling between eIF4G and eIF4E. Cell 115, 739–750.
[43] Ptushkina, M., von der Haar, T., Vasilescu, S., Frank, R., Birkenhager, R. and McCarthy, J.E. (1998) Cooperative modulation by eIF4G of eIF4E-binding to the mRNA 5′ cap in yeast involves a site partially shared by p20. EMBO J. 17, 4798–4808.
[44] Slepenkov, S.V., Korneeva, N.L. and Rhoads, R.E. (2008) Kinetic mechanism for assembly of the m7G pppG·eIF4E·eIF4G complex∗S. J. Biol. Chem. 283, 25227–25237.
[45] Thoreen, C.C., Chantranupong, L., Keys, H.R., Wang, T., Gray, N.S. and Sabatini, D.M. (2012) A unifying model for mTORC1-mediated regulation of mRNA translation. Nature 485, 109–113.